

Tumor-associated tertiary lymphoid structure predicts postoperative outcomes in patients with primary gastrointestinal stromal tumors

Qiaowei Lin^{a*}, Ping Tao^{b*}, Jiongyuan Wang^{a,c*}, Lijie Ma^c, Quan Jiang^a, Jinglei Li^a, Ge Zhang^a, Ju Liu^d, Yong Zhang^{a,c}, Yingyong Hou^d, Weiqi Lu^{a,c}, Ruyi Xue^e, and Hanxing Tong^{a,c*}

^aDepartment of General Surgery, Zhongshan Hospital, Fudan University, Shanghai, China; ^bDepartment of Laboratory Medicine, Shanghai TCM-integrated Hospital, Shanghai University of Traditional Chinese Medicine, Shanghai, China; ^cDepartment of General Surgery, Zhongshan Hospital (South), Shanghai Public Health Clinical Center, Fudan University, Shanghai, China; ^dDepartment of Pathology, Zhongshan Hospital, Fudan University, Shanghai, China; ^eDepartment of Gastroenterology and Hepatology, Zhongshan Hospital, Fudan University, Shanghai, China

ABSTRACT

Tumor-infiltrating tertiary lymphoid structures (TLS) are thought to have anti-tumor activity and are believed to indicate a favorable prognosis in cancer patients. However, the prognostic value of TLS in gastrointestinal stromal tumors (GIST) is unknown. We evaluated the prognostic value of TLS using two independent GIST cohorts. Pathological examinations identified TLS in 44.9% of patients in our discovery cohort (DC). TLS was significantly associated with smaller tumor size ($P = .011$), relatively well morphological classification ($P < .001$), lower NIH classification ($P < .001$), lower recurrence ($P = .005$), longer survival time ($P < .001$) and lower imatinib resistance ($P = .006$). Kaplan-Meier curves showed that TLS was remarkably associated with favorable survival ($P = .0002$) and recurrence ($P = .0015$) time. In addition, the presence of *KIT* mutations and the absence of TLS suggested worst prognosis both in terms of overall survival (OS) ($P = .0029$) and time to recurrence (TTR) ($P = .0150$), while the presence of *PDGFRA* mutations and TLS suggested optimal prognosis for OS and TTR. Multivariate analyses demonstrated that TLS was an independent prognostic factor for OS (HR:0.180, $P = .002$) and TTR (HR:0.412, $P = .023$). These results were confirmed using our validation cohort. Multiplexed immunohistochemistry staining was used to determine the composition of TLS. Therapies designed to target TLS may be a novel therapeutic strategy for GIST patients with imatinib resistance.

ARTICLE HISTORY

Received 13 September 2019
Revised 8 January 2020
Accepted 20 January 2020

KEYWORDS

Tertiary lymphoid structure (TLS); gastrointestinal stromal tumor (GIST); immune microenvironment; prognosis; imatinib

Introduction

Gastrointestinal stromal tumors (GIST) are the most common sarcomas of the digestive tract.¹ The annual incidence is approximately 5000 in the United States.² GISTs are thought to be derived from interstitial cells of the Cajal, pacemaker cells of the intestine or their precursors.³ GIST occurs most frequently in the stomach (60%), followed by the small intestine (25–35%) and colon (5%).^{1,4,5} Activating mutations in *KIT* are present in 75–80% of patients, while 5–10% of patients harbor mutations in platelet-derived growth factor receptor alpha (*PDGFRA*).^{6,7} Imatinib, a tyrosine kinase inhibitor first used in metastatic GIST in 2001 with a great success,⁸ has dramatically improved the prognosis of GIST patients, with 80% clinical response.^{9,10} However, imatinib was never curative for GIST. Probably due to secondary *KIT* or *PDGFRA* mutations, resistance often developed within 18 months of imatinib administration.^{11,12} Sunitinib¹³ or regorafenib¹⁴ would then be recommended. However, their efficacy would last only for a few months. Hence, it is critical to find new treatment strategies to overcome resistance and treat patients with unresectable GIST.

The immune microenvironment plays an important role in the development of various tumors. Tertiary lymphoid structures (TLS) are ectopic lymphoid formations found in patients during chronic infections, graft rejections, autoimmune diseases, and tumors.¹⁵ They consist of a T cell zone with a high density of DC-Lamp⁺ mature dendritic cells (DC) and a B cell follicular zone.¹⁶ TLS may act as a nest for recruiting lymphocytes from the blood^{17–19} or have an anti-tumor role.¹⁶ TLS has been associated with a favorable prognosis in most solid cancers, including non-small cell lung cancer (NSCLC),²⁰ pancreatic cancer,²¹ colorectal cancer (CRC),¹⁹ breast cancer²² and melanomas.²³ Intra-tumoral TLS have been associated with positive clinical outcomes in patients with hepatocellular carcinomas, while peri-tumoral TLS have not.²⁴ However, the role of TLS in GIST had not been fully elucidated.

Using hematoxylin-eosin (H&E) staining, the prognostic significance of TLS in 187 patients with primary GIST treated with surgical resection was evaluated. These 187 patients were randomly divided into a discovery cohort (DC) with 118 patients and a validation cohort (VC) with 69 patients. We demonstrated that TLS was associated with lower future

CONTACT Ruyi Xue  xue.ruyi@zs-hospital.sh.cn  Department of Gastroenterology and Hepatology, Zhongshan Hospital, Fudan University, Shanghai 200030, China; Hanxing Tong  tong.hanxing@zs-hospital.sh.cn; Weiqi Lu  lu.weiqi@zs-hospital.sh.cn  Department of General Surgery, Zhongshan Hospital, Fudan University, Shanghai 200030, China

*These authors contributed equally to this work.

 Supplemental data for this article can be accessed on the [publisher's website](#).

© 2020 The Author(s). Published with license by Taylor & Francis Group, LLC.

This is an Open Access article distributed under the terms of the Creative Commons Attribution-NonCommercial License (<http://creativecommons.org/licenses/by-nc/4.0/>), which permits unrestricted non-commercial use, distribution, and reproduction in any medium, provided the original work is properly cited.

imatinib resistance, longer survival time and recurrence time and was an independent prognostic factor in patients with GIST.

Materials and methods

Patients and GIST samples

Two independent primary GIST patient cohorts (DC: n = 118; VC: n = 69) who underwent radical resections at Zhongshan Hospital of Fudan University between 2009 to 2014 were retrospectively reviewed and enrolled in this study. All patients did not receive imatinib prior to their surgery. Clinicopathologic features were not significantly different between the two cohorts (Supplementary Table S1). Informed signed written consent was obtained from each patient. Ethical approval was obtained from the Research Ethics Committee of Zhongshan Hospital (B2012-022).

Hematoxylin and eosin staining

Tumor samples were fixed in 4% paraformaldehyde solution and embedded in paraffin. GIST samples were then sliced into 4 μ m sections. Deparaffinization and rehydration of the tissues were performed using xylene and ethanol respectively, followed by hematoxylin staining for 5 minutes and 1% acid ethanol for 3 seconds. The sections were then rinsed in distilled water and stained with eosin for 3 minutes. Dehydration and hyalinization were then subsequently performed. Sections were scanned using an automatic digital slide scanner Panoramic MIDI (3DHISTECH, Hungary) and analyzed using the CaseViewer (3DHISTECH, Hungary).

Pathological examinations

The diagnosis was confirmed by two independent pathologists specialized in GIST in our institute. The following pathological features were recorded: primary tumor location, tumor size, mitosis rate, nuclear atypia, morphological classification, morphology, NIH classification, Ki67 and mutations. Morphological classifications were based on the criteria proposed by Professor Hou at our hospital.²⁵

Multiplexed immunohistochemistry staining

Multiplexed immunohistochemistry staining was performed in some of the tumor samples. The samples were fixed in 4% paraformaldehyde solution and embedded in paraffin. Slides were made using 4 μ m sections of the tumor samples. Deparaffinization and rehydration were performed with xylene and ethanol respectively, followed by microwave antigen retrieval using heated citric acid buffer (pH 6.0) for 10 minutes and endogenous peroxidase blocking in 3% H₂O₂ for 20 minutes. Goat serum (Vector, MP-7451) was used to block nonspecific binding sites. Afterward, relevant primary antibodies were incubated for 1 hour at room temperature, followed by the corresponding secondary antibodies (Vector, MP-7451; MP-7452) for 20 minutes. Slides were then incubated with fluorescein TSA plus for 10 minutes, after which microwave antigen retrieval was

repeated with the above steps until the last antibody was added. After multiplexing, DAPI (Sigma, D9542) was used to stain the nuclei. Antibodies and fluorescent dyes used for multiplexing are listed in Supplementary Table S2. The slides were scanned by Vectra 3 automated high-throughput multiplexed biomarker imaging system (Perkin Elmer) and analyzed using the inform image analysis software (Perkin Elmer). Immune cells were classified into the following types: Regulatory T cells (Treg) (CD4⁺Foxp3⁺), Th1 cells (CD4⁺T-Bet⁺), Th2 cells (CD4⁺GATA3⁺), Th17 cells (CD4⁺ROR γ t⁺), CD8⁺T cells (CD8⁺), Tissue-resident memory T cells (Trm) (CD103⁺), plasma cells (PCs) (CD20⁻CD24⁻CD27^{hi}CD38^{hi}), B cells (CD20⁺), naive B cells (Bn) (CD20⁺CD27⁻IgM⁺), IgM⁺ memory B cells (IgM⁺ Bm) (CD20⁺CD27⁺IgM⁺), CD27⁻ isotype-switched memory B cells (CD27⁻ Sw Bm) (CD20⁺CD27⁻IgM⁺), and CD27⁺ isotype-switched memory B cells (CD27⁺ Sw Bm) (CD20⁺CD27⁺IgM⁺).

Statistical analysis

Statistical analyzes were performed using the IBM SPSS Statistics 23 (SPSS Inc., Armonk, NY, USA) and GraphPad Prism 7.0 (GraphPad Software, La Jolla, CA, USA) software. Pearson chi-square test was used to analyze the relationship between TLS and qualitative variables and Fisher's exact test was used when necessary. Multivariate analyzes were performed using Cox proportional hazards regression to identify independent prognostic factors. Kaplan-Meier analysis was used to compare differences after curative surgery for patient overall survival (OS) and time to recurrence (TTR). *P*-value <0.05 was considered statistically significant.

Results

Patient characteristics and TLS status

Detailed patient clinical characteristics are shown in Supplementary Table S1. There were 118 and 69 patients in our DC and VC respectively. 61% of the patients were male in the DC and 52% in the VC. 52% of the patients in the DC were above 60 years old, while 48% of the patients were above 60 years old in the VC. For patients in the DC, tumors were mostly located in the stomach (52%), followed by the small intestine (39%) and others (9%), and was similar to the VC. Most patients (approximately 78%) had tumors larger than 5 cm in both the cohorts, probably because that physical examinations were not popularized in China. Postoperative National Institutes of Health (NIH) classification indicated that high-risk patients were the majority, followed by low risk and medium risk patients. With regards to mutational status, most tumors had *KIT* mutations (83%), followed by *PDGFRA* mutations (about 10%) and wide type (WT) (about 7%) which were relatively less common in our cohorts and was consistent with previous reports. 69 patients in the DC were administered imatinib with 19 (27.5%) developing drug resistance. For patients in the VC, imatinib resistance occurred in 38.1% of 42 patients. Relapse and death occurred in 47 (39.8%) and 24 (20.3%) of patients in the DC respectively, and 25 (36.2%) and 16 (23.2%) of patients in the VC.

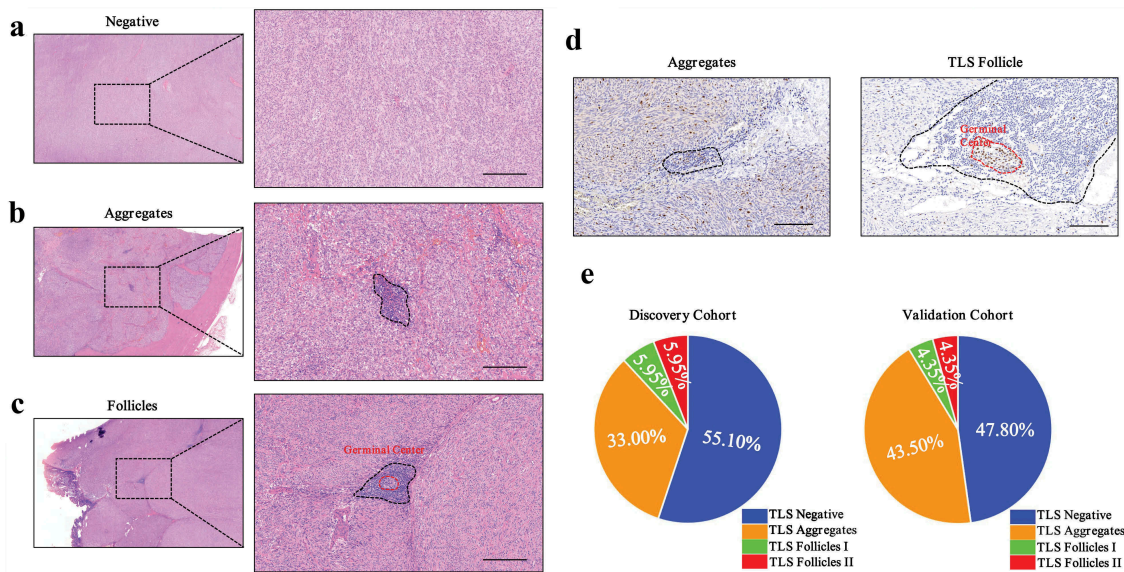


Figure 1. The classification of tertiary lymphoid structure (TLS) in primary GIST.

(a). Representative H&E image of TLS⁻ patients. Scale bar: 40 μm (left); 200 μm (right)(b). Representative H&E image of TLS Aggregates patients. (black dotted portion: TLS aggregates). Scale bar: 40 μm (left); 200 μm (right)(c). Representative H&E image of TLS FollICLES patients. (black dotted portion: TLS FollICLES; red dotted portion: germinal center). Scale bar: 40 μm (left); 200 μm (right)(d). Typical IHC staining of Ki67 in germinal center. (left: TLS aggregates; right, TLS FollICLES). Scale bar: 400 μm.(e). TLS phenotype and frequency evaluated in discovery (left) and validation cohort (right). Proportions of TLS⁻, TLS Aggregates, Follicle I and Follicle II in GIST were summarized by pie chart.

Tumor-infiltrating TLS were classified into three categories based on their morphology determined by H&E staining; 1) TLS⁻: no clusters of lymphocytes (Figure 1a); 2) TLS Aggregates (Agg): small, quasi-circular clusters of lymphocytes (Figure 1b); 3) TLS FollICLES (FL): large clusters with (FL-II) or without (FL-I) germinal center formation (Figure 1c). Ki-67 staining additionally confirmed the presence of a germinal center (Figure 1d). We defined tumors with no TLS as TLS⁻ and tumors with one or more TLS as TLS⁺. Based on the classification criterion described above, we identified TLS in 53 tumors (44.9%), of which 39 patients (33%) were TLS Agg, 7 patients (5.95%) were TLS FL-I and 7 patients (5.95%) were TLS FL-II in our DC (Figure 1e). In the VC, 33 patients (47.8%) and 36 patients (52.2%) were classified as TLS negative and positive respectively and consisted of 30 TLS Agg (43.5%) patients, 3 TLS FL-I (4.35%) patients and 3 TLS FL-II (4.35%) patients.

TLS immune profiles in GIST patients

To get a better understanding of TLS, we investigated the general composition of TLS in GIST patients using multiplexed immunohistochemistry staining. We found that TLS consisted of a CD4⁺ or CD8⁺ T cell zone in the outer layer and a CD20⁺ B cell zone in the inner layer (Figure 2a). As for the specific immune cell subtypes, the TLS was mostly composed of CD4⁺ T cells, CD8⁺ T cells, Trm cells, and CD20⁺ B cells, while a relatively small percentage of Treg cells, Th1 cells, Th2 cells, Th17 cells, PCs, Bn cells, IgM⁺ Bm cells, CD27⁻ Sw Bm cells and CD27⁺ Sw Bm cells were observed (Figure 2a). Trm cells were mostly localized in the outer layer of the TLS and were relatively close to tumor cells, which indicated that they may play a vital role in anti-tumor response.²⁶ Th2 cells were close to the B cell zone, which

may be beneficial for the interaction of cellular and humoral immunity.²⁷ PCs were mostly located around the follicles, suggesting antibody production *in situ*.²⁸ However, the distribution of other cells, including Treg cells, Th1 cells, Th17 cells, Bn cells, IgM⁺ Bm cells, CD27⁻ Sw Bm cells and CD27⁺ Sw Bm cells, had no characteristic localization patterns.

Heterogeneity of immune profiles between TLS⁺ and TLS⁻ GIST patients

To better understand the differences in immune profiles between TLS⁺ and TLS⁻ patients, we performed multiplexed immunohistochemistry staining. Surprisingly, we found that TLS⁻ patients had a higher number of Treg cells and a lower number of B cells in the tumor area (Figure 2b,c). This may partly explain why TLS⁻ patients had poor OS and TTR. However, we did not observe any differences in the number of CD8⁺ or CD4⁺ T cells (Supplementary Figure 1A).

Correlation between TLS and clinicopathological features in GIST patients

To evaluate the clinical importance of TLS in GIST, patients were divided into TLS⁺ and TLS⁻ groups. The association between clinicopathological features and the selected variables are summarized in Table 1. The presence of TLS was positively correlated with smaller tumor size (DC, $P = .011$; VC, $P = .008$), relatively well defined morphological classifications ($P < .001$ for both cohort), lower NIH classification (DC, $P < .001$; VC, $P = .005$), lower possibility to develop drug resistance (DC, $P = .007$; VC, $P = .020$), recurrence (DC, $P = .005$; VC, $P = .003$) and favorable survival (DC, $P < .001$; VC, $P = .004$). However, the relationship between

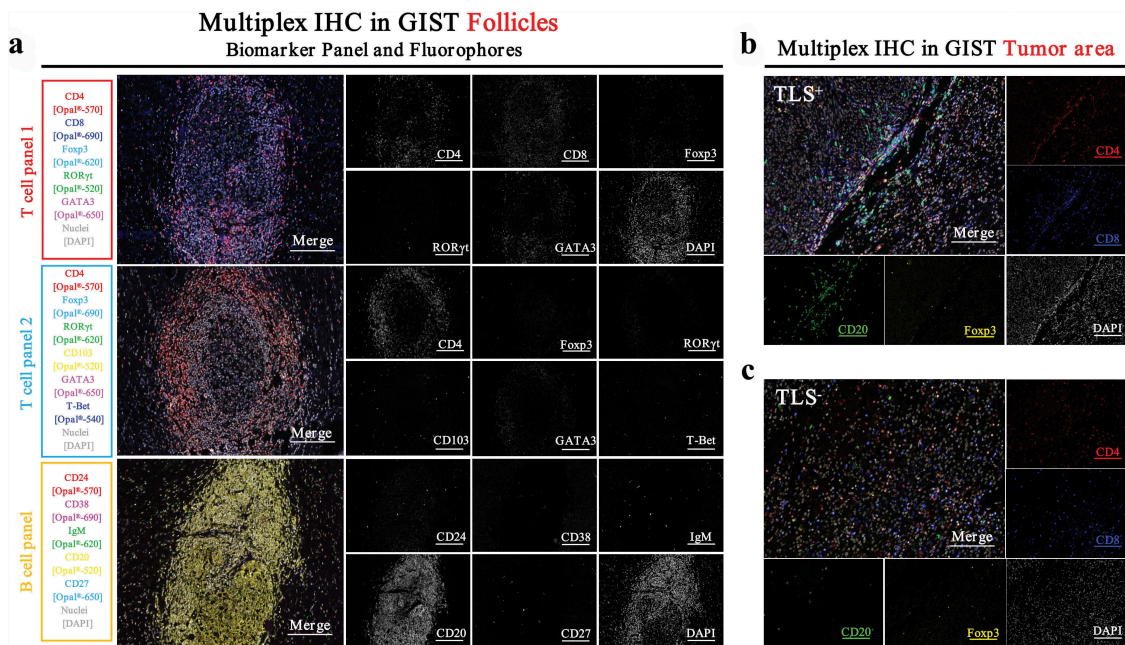


Figure 2. Immune profiles of TLS in GIST defined by multiplexed immunohistochemistry staining.

(a). Representative 7-plex immunofluorescence image of T and B patterns of TLS follicles. Composite image (left) showing the colocalization staining pattern and the right panel shows a single-channel along. T cell panel 1 to show Treg cells ($CD4^+Foxp3^+$), Th17 cells ($CD4^+ROR\gamma^+$), Th2 cells ($CD4^+GATA3^+$) and $CD8^+$ T cells ($CD8^+$). T cell panel 2 to show T_{RM} cells ($CD103^+$), Treg cells ($CD4^+Foxp3^+$), Th17 cells ($CD4^+ROR\gamma^+$), Th2 cells ($CD4^+GATA3^+$) and Th1 cells ($CD4^+T-bet^+$). B cell panel to show plasma cells (PCs) ($CD20^+CD24^-CD27^{hi}CD38^{hi}$), B cells ($CD20^+$), naive B cells (Bn) ($CD20^+CD27^-IgM^+$), IgM⁺ memory B cells (IgM⁺ Bm) ($CD20^+CD27^+IgM^+$), $CD27^-$ isotype-switched memory B cells ($CD27^- Sw Bm$) ($CD20^+CD27^-IgM^-$) and $CD27^+$ isotype-switched memory B cells ($CD27^+ Sw Bm$) ($CD20^+CD27^+IgM^-$). Scale bars, 200 μ m. (b). Representative images of five-color multiplex present immune profile in TLS^+ patients, Scale bar: 200 μ m. (c). Representative images of five-color multiplex present immune profile in TLS^- patients, Scale bar: 200 μ m.

TLS and mitotic index (DC, $P = .041$; VC, $P = .161$) or mutational status were only significantly different in the DC ($P = .011$; VC, $P = .056$) but not in the VC. This may be due to the relatively small sample size in our VC.

TLS predicts future imatinib resistance

Resistance to imatinib usually occurs after GIST therapy. Hence, patients in the DC and VC who were administered imatinib after surgery were selected to determine whether imatinib resistance was associated with TLS. Surprisingly, we found that most patients who developed imatinib resistance were TLS^- (Figure 3a,b), however, there were no differences in the number of TLS^- or TLS^+ patients who did not develop resistance (Table 3, Figure 3b). Interestingly, patients categorized with TLS Follicles never developed imatinib resistance in both the DC and VC (Figure 3b). This suggested that TLS maturity may correlate with future imatinib resistance. Furthermore, we found that TLS^- patients were more likely to develop drug resistance in the future (DC, $P = .006$; VC, $P = .014$), which may suggest that the immune system in these patients may play a protective role in preventing imatinib resistance (Table 2). In addition, imatinib resistance was significantly associated with clinical outcomes of recurrence ($P < .0001$ in both cohorts) and death ($P < .0001$ in both cohorts) (Table 2).

We then analyzed the relationship between drug-resistant time and TLS phenotype. We observed that TLS^+ patients had longer drug-resistant times compared to TLS^- patients (DC, $P = .0075$; VC, $P = .0171$) (Figure 3c).

To determine the cell type that may contribute to future imatinib resistance, we analyzed the composition of TLS between imatinib-resistant and nonresistant patients. Interestingly, we found that imatinib-resistant patients had more Treg cells and $CD20^+$ B cells and lower $CD8^+$ T cells in the TLS (Supplementary Figure 1B and 1C). This suggested that Treg cells and $CD20^+$ B cells may contribute to imatinib resistance while a lower number of $CD8^+$ T cells may be a risk factor of future imatinib resistance. However, we did not observe any differences in the number of $CD4^+$ T cells (Supplementary Figure 1B and 1C).

Prognostic significance of TLS in GIST patients

To evaluate the prognostic value of TLS in GIST patients, Kaplan-Meier curves were performed. We observed that TLS^+ patients had better OS (DC, $P = .0002$; VC, $P = .0019$) and TTR (DC, $P = .0015$; VC, $P = .0021$) compared to TLS^- patients (Figure 4a,b, left). Furthermore, significant differences in survival and recurrence were observed in Agg, FL-I and FL-II TLS subgroups (Figure 4a,b, right). In the DC, the median OS and TTR were 66 months and 53 months for TLS^- Agg, 74 months and 68 months for TLS^- FL-I, and 94 months and 78 months for TLS^- FL-II.

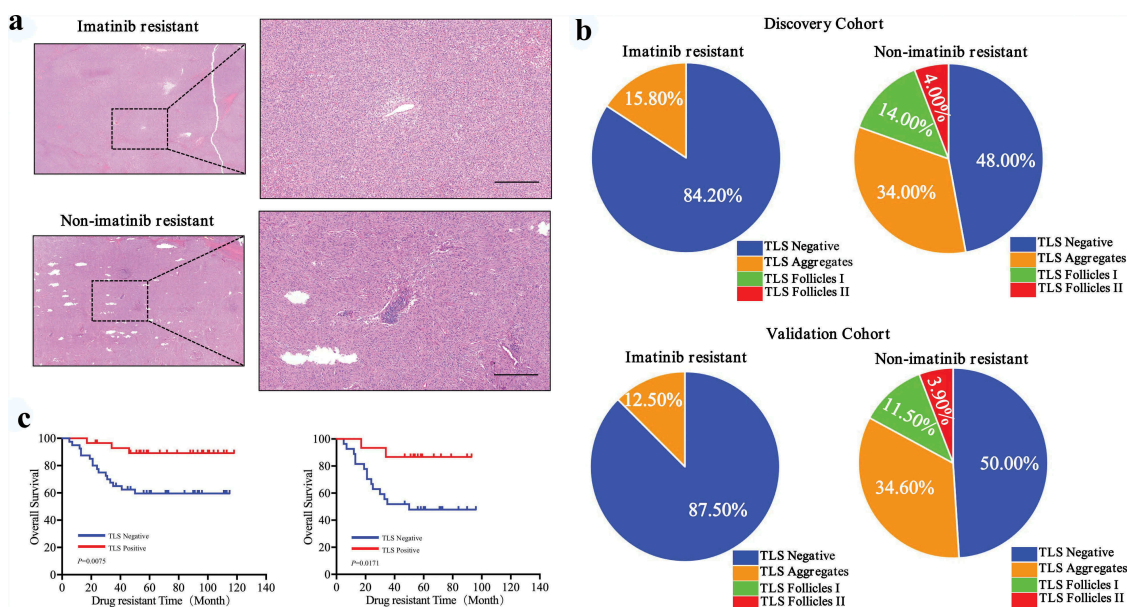
To further exclude the possible impact of imatinib, multivariate cox regression analyzes were performed, which indicated that imatinib was not an independent factor for OS and TTR (OS: DC, HR:0.676, $P = .443$; VC, HR:0.958, $P = .953$) (TTR: DC, HR:0.486, $P = .084$; VC, HR:0.868, $P = .817$) (Table 3). In

Table 1. The correlation between TLS and clinicopathological features in whole series (n = 187).

Variables	Discovery cohort (n = 118)			Validation cohort (n = 69)		
	TLS ⁺	TLS ⁻	P*	TLS ⁺	TLS ⁻	P*
Gender (Male vs. Female)	41/24	31/22	0.611	21/15	15/18	0.285
Age (years) (≤60 vs. >60)	32/33	29/24	0.553	20/16	19/14	0.866
Site (Gastric vs. Small intestine vs. Others)	34/27/4	27/19/7	0.413	19/14/3	17/12/4	0.982
Tumor size (cm) (≤5 vs. >5)	20/45	6/47	0.011	13/23	3/30	0.008
Mitotic index (/50HPF) (≤5 vs. >5)	29/36	14/39	0.041	18/18	11/22	0.161
Nuclear atypia (Mild vs. Moderate or Distinct)	44/21	28/25	0.100	25/11	23/10	0.982
Morphological classification (Low vs. Borderline vs. High)	24/23/18	7/10/35	<0.001	6/17/13	3/3/27	<0.001
Morphology (Spindle vs. Epithelioid vs. Mixed)	44/9/12	41/3/8	0.288	23/4/9	26/2/5	0.393
NIH classification (Low vs. Medium vs. High)	15/4/46	1/1/51	<0.001	10/4/22	1/1/31	0.005
Mutation (<i>KIT</i> vs. <i>PDGFRA</i>)	50/11	48/1	0.011	27/7	30/1	0.056
(<i>KIT</i> vs. WT)	50/4	48/4	>0.999	27/2	30/2	>0.999
(<i>PDGFRA</i> vs. WT)	11/4	1/4	0.109	7/2	1/2	0.236
Ki67 (%) [#] (<5 vs. ≥5)	25/25	17/25	0.361	14/14	8/16	0.225
Drug resistance (Yes vs. No)	3/26	16/24	0.007	2/13	14/13	0.020
Recurrence (Yes vs. No)	18/47	29/24	0.005	7/29	18/15	0.003
Death (Yes vs. No)	5/60	19/34	<0.001	3/33	13/20	0.004

Abbreviation: NIH, National Institutes of Health; *PDGFRA*, Platelet-derived growth factor receptor alpha; WT, Wide Type. Pearson chi-square tests or Fisher's exact tests for all the other analysis.

[#] Available in 92 cases in discovery cohort and 52 cases in validation cohort.

**Figure 3.** Differences of TLS phenotype between imatinib resistant patients and non-imatinib resistant patients.

(a). Representative H&E images in imatinib resistant (upper panel) and non-imatinib resistant patients (bottom panel). Scale bar: 40 μm (left); 200 μm (right). (b). Proportions of TLS⁻, Aggregates, Follicle I and Follicle II in our discovery cohort (upper panel) and validation cohort (bottom panel). (c). Kaplan-Meier curves of drug resistant time in patients with TLS⁺ and TLS⁻ (left, discovery cohort; right, validation cohort).

addition, we analyzed the OS and TTR in patients who had a history of imatinib usage after surgery. Similar results were observed and were summarized in Figure 5.

We then analyzed the number, density, and location of TLS. The presence of TLS was associated with a better OS and TTR, no matter located in the tumor or peri-tumor region (Supplementary Figure 2). With regards to the number and density of TLS, we observed that patients with a large number or high density of TLS had a better OS and TTR compared to patients with small number or low density of TLS (Supplementary Figure 3).

In addition, univariate cox regression analyzes for the two cohorts were performed. We observed that age (DC,

HR:3.628, $P = .006$; VC, HR:3.204, $P = .031$), mitotic index (DC, HR:4.619, $P = .013$; VC, HR:6.515, $P = .013$) and TLS (DC, HR:0.181, $P = .001$; VC, HR:0.172, $P = .006$) were significantly associated with OS in GIST (Table 3). Multivariate cox regression analyzes identified age (DC, HR:3.502, $P = .014$; VC, HR:3.167, $P = .035$) and TLS (DC, HR:0.180, $P = .002$; VC, HR:0.219, $P = .030$) as independent prognostic factors for OS (Table 3).

With regards to TTR, univariate cox regression analyzes identified primary tumor location (DC, HR:2.015, $P = .001$; VC, HR:2.278, $P = .003$), tumor size (DC, HR:2.908, $P = .024$; VC, HR:4.261, $P = .049$), mitotic index (DC, HR:4.875, $P < .001$; VC, HR:7.315, $P = .001$), morphology classification

Table 2. The correlation between imatinib resistance and clinicopathological features.

Variables	DC drug resistance			VC drug resistance		
	No	Yes	<i>P</i> *	No	Yes	<i>P</i> *
Gender(Male vs. Female)	28/22	13/6	0.348	13/13	10/6	0.429
Age (years)(≤60 vs. >60)	28/22	8/11	0.302	18/8	7/9	0.102
Site(Gastric vs. Small intestine vs. Others)	25/21/4	6/7/6	0.051	11/14/1	5/6/5	0.064
Tumor size (cm)(≤5 vs. >5)	9/41	2/17	0.449	3/23	2/14	1.000
Mitotic index (/50HPF)(≤5 vs. >5)	12/38	3/16	0.534	7/19	3/13	0.715
Nuclear atypia(Mild vs. Moderate or Distinct)	26/24	11/8	0.661	17/9	10/6	0.850
Morphological classification(Low vs. Borderline vs. High)	8/13/29	2/1/16	0.107	1/4/21	2/0/14	0.196
Morphology(Spindle vs. Epithelioid vs. Mixed)	39/3/8	13/2/4	0.641	25/0/5	11/2/3	0.286
NIH classification(Low vs. Medium vs. High)	3/0/47	0/0/19	0.556	1/0/25	0/0/16	1.000
Mutation(<i>KIT</i> vs. <i>PDGFRA</i> vs. WT)	48/0/2	66/1/2	0.330	25/0/1	15/1/0	0.623
Ki67 (%)#(<5 vs. ≥5)	16/24	3/10	0.330	6/15	3/8	1.000
TLS(Positive vs. Negative)	26/24	3/16	0.006	13/13	2/14	0.014
Recurrence(Yes vs. No)	37/13	19/0	<0.001	22/4	16/0	<0.001
Death(Yes vs. No)	4/46	13/6	<0.001	0/26	13/3	<0.001

Abbreviation: NIH, National Institutes of Health; *PDGFRA*, Platelet-derived growth factor receptor alpha; WT, Wide Type.

*Pearson chi-square tests or Fisher's exact tests for all the other analysis.

Available in 92 cases in discovery cohort and 52 cases in validation cohort.

(DC, HR:1.847, $P = .003$; VC, HR:2.285, $P = .030$), drug resistance (DC, HR:16.833, $P < .001$; VC, HR:41.974, $P < .001$) and TLS (DC, HR:0.397, $P = .002$; VC, HR:0.278, $P = .004$) as clinicopathologic factors that correlated with TTR (Table 3). Furthermore, multivariate analyzes identified that mitotic index (DC, HR:7.872, $P = .014$; VC, HR:9.684, $P = .002$) and TLS (DC, HR:0.412, $P = .023$; VC, HR:0.193, $P = .002$) were independent indicators for TTR (Table 3).

We then evaluated the prognostic value of TLS phenotypes in both our cohorts (the combination of discovery and validation cohorts). Our results demonstrated that the presence of TLS was a valuable prognostic factor for post-operative survival in GIST patients, no matter located in the tumor or peritumor region (Supplementary Figure 4 and 5).

Mutational status combined with TLS predicts future clinical outcomes

Mutational status has been the hallmark for most GIST patients.²⁹ Hence, we analyzed the relationship between mutational status and TLS. Differences in TLS morphology were not found in patients with *KIT* mutations (Figure 6a), *PDGFRA* mutations (Figure 6b) and WT genotypes (Figure 6c). We then analyzed the percentages of TLS⁺ patients with different mutations and observed that patients with *PDGFRA* mutations were more likely to have TLS compared to patients with *KIT* mutations or WT genotypes (Figure 6d). Kaplan-Meier curves were then generated based on the combination of mutational and TLS status. Patients were categorized into three groups (Group I, *KIT* mutations and TLS⁻; Group III, *PDGFRA* mutations and TLS⁺; Group II, others). Significant differences in survival and recurrence were observed for the different subgroups. Group III had the best prognosis for OS ($P = .0029$) and TTR ($P = .0150$) while Group I had the worst prognosis (Figure 6e). Similar results were observed in our validation cohort (Figure 6f).

Discussion

The tumor microenvironment had been intensely investigated in recent years, especially the immune microenvironment.

TLS provides a local and essential microenvironment for both the innate and acquired immune system to eliminate tumor cells.³⁰ It is considered an indicator of favorable clinical outcomes in virtually most patients with solid tumors.^{31,32} TLS has been demonstrated to orchestrate a Th1 cell-polarized and cytotoxic CD8⁺ T cell anti-tumor immune response in NSCLC.³³ In addition, TLS has been associated with lymphatic invasion, increased pathological nodal stages and nodal involvement in some tumors.³⁴ TLS has even been detected in metastases in parallel with primary tumors.³⁵ In addition, the presence of TLS with desmoplastic melanomas have a higher response rate to PD-1 blockade.³⁶ High proportions of regulatory T cells (Treg) in TLS are thought to control the extent and activation of CD4⁺ and CD8⁺ T cell infiltrates and correlate with poor prognosis³⁷ whereas depletion of Treg cells leads to exacerbation of the disease and increased tumor infiltration by CD4⁺ and CD8⁺ T cells and macrophages.³⁸

In the present study, we demonstrate for the first time that the presence of TLS in GIST correlated with favorable tumor characteristics, including smaller tumor size, well morphological classifications, lower NIH classifications, and lower imatinib resistance. This indicated that TLS may contribute to effective anti-tumoral immune responses by promoting local antigen presentation and lymphocyte differentiation. Mature dendritic cells (DCs) present antigens to CD4⁺ T cells to activate cellular immunity in the T cell zone,³⁹ while DC-LAMP⁺ DCs in the germinal center present antigens to B cells to induce humoral immunity.⁴⁰ B cells could also present antigens to CD8⁺ T cells, possibly through CD80 and CD40 receptors on B cells. This replaces the need for CD4⁺ T cells to transmit signals to CD8⁺ T cells for anti-tumor responses.⁴¹⁻⁴³ Interestingly, intravenous injection of GFP splenocytes in mouse models results in the homing of lymphocytes to the TLS. This suggests an active role of TLS in the recruitment of lymphocytes to tumor regions,¹⁹ and may partly explain our findings.

To gain a better understanding of TLS in GIST patients, we performed multiplexed immunohistochemistry staining. TLS was mostly composed of a T cell zone in the outer layer and a B cell zone in the inner layer. With regards to immune cell subtypes, CD4⁺ T cells, CTL, Trm cells and CD20⁺ B cells

Table 3. Univariate and multivariate analyses of clinicopathological features and overall survival and time to recurrence in whole series (n = 187).

Variable	Discovery cohort (n = 118)			Validation cohort (n = 69)		
	OS		TTR	OS		TTR
	HR (95%CI)	P	HR (95%CI)	P	HR (95%CI)	P
Univariate analysis						
Gender						
Male vs. Female	0.754(0.322–1.761)	0.514	0.630(0.337–1.179)	0.148	0.617(0.224–1.700)	0.351
Age (years)						
≤60 vs. >60	3.628(1.440–9.143)	0.006	1.743(0.973–3.122)	0.062	3.204(1.113–9.223)	0.031
Site						
Gastric vs. Small intestine vs. Others	2.045(1.165–3.588)	0.013	2.015(1.341–3.027)	0.001	1.785(0.899–3.546)	0.098
Tumor size (cm)						
≤5 vs. >5	3.455(0.812–14.697)	0.093	2.908(1.149–7.355)	0.024	2.404(0.546–10.594)	0.246
Nuclear abnormalities						
Mild vs. Moderate or Distinct	2.269(1.007–5.109)	0.048	1.630(0.919–2.892)	0.095	1.794(0.666–4.828)	0.247
Mitotic index (/50HPP)						
≤5 vs. >5	4.619(1.377–15.495)	0.013	4.875(2.067–11.497)	<0.001	6.515(1.474–28.792)	0.013
Morphology classification						
Low vs. Borderline vs. High	2.319(1.235–4.354)	0.009	1.847(1.237–2.759)	0.003	1.916(0.791–4.642)	0.150
Morphology						
Spindle vs. Epithelioid vs. Mixed	1.212(0.743–1.979)	0.441	0.892(0.601–1.323)	0.570	1.046(0.569–1.923)	0.885
NIH classification						
Low and Medium vs. High	6.625(0.544–80.665)	0.138	3.988(1.328–11.978)	0.014	8.037(0.473–136.677)	0.149
Postoperative imatinib treatment						
Yes vs. No	1.802(0.747–4.348)	0.190	1.575(0.853–2.909)	0.147	3.220(0.914–11.342)	0.069
Ki67 (%)#						
<5 vs. ≥5	2.126(0.749–6.037)	0.157	2.640(1.269–5.493)	0.009	1.538(0.463–5.112)	0.482
Mutation						
KIT vs. PDGFRA vs. WT	0.849(0.329–2.189)	0.735	0.833(0.424–1.637)	0.596	1.097(0.354–3.394)	0.873
KIT vs. Non-KIT	2.422(0.569–10.304)	0.231	2.386(0.856–6.651)	0.096	3.488(0.460–26.450)	0.227
PDGFRA vs. Non-PDGFRA	0.039(0.000–5.835)	0.205	0.123(0.017–0.895)	0.038	0.039(0.000–15.470)	0.287
Drug resistance						
Yes vs. No	13.132(4.255–40.527)	<0.001	16.833(6.869–41.251)	<0.001	363.123(0.884–149227.953)	0.055
TLS						
Positive vs. Negative	0.181(0.067–0.484)	0.001	0.397(0.220–0.719)	0.002	0.172(0.049–0.606)	0.006
Multivariate analysis						
Age (years)						
≤60 vs. >60	3.502(1.295–9.474)	0.014	NA	NA	3.167(1.088–9.223)	0.035
Site						
Gastric vs. Small intestine vs. Others	1.678(0.942–2.989)	0.079	1.796(1.055–3.057)	0.031	NA	NA
Tumor size (cm)						
≤5 vs. >5	NA	NA	2.154(0.674–6.888)	0.196	NA	NA
Nuclear abnormalities						
Mild vs. Moderate or Distinct	1.071(0.459–2.499)	0.875	NA	NA	NA	NA
Mitotic index (/50HPP)						
≤5 vs. >5	3.373(0.915–12.433)	0.068	7.872(1.517–40.854)	0.014	5.134(1.091–24.165)	0.038
Morphology classification						
Low vs. Borderline vs. High	0.879(0.414–1.867)	0.737	0.879(0.505–1.531)	0.649	NA	NA
NIH classification						
Low vs. Medium vs. High	NA	NA	1.156(0.332–4.025)	0.820	NA	NA
Postoperative imatinib treatment						
Yes vs. No	0.676(0.249–1.839)	0.443	0.486(0.214–1.102)	0.084	0.958(0.233–3.936)	0.953
Ki67 (%)#						
<5 vs. ≥5	NA	NA	1.346(0.604–2.997)	0.467	NA	NA
TLS						
Positive vs. Negative	0.180(0.061–0.534)	0.002	0.412(0.192–0.887)	0.023	0.219(0.056–0.862)	0.030

Abbreviation: NIH, National Institutes of Health; PDGFRA, Platelet-derived growth factor receptor alpha; WT, Wide Type.

Cox regression analyses were done for all the above data.

Available in 92 cases in discovery cohort and 52 cases in validation cohort.

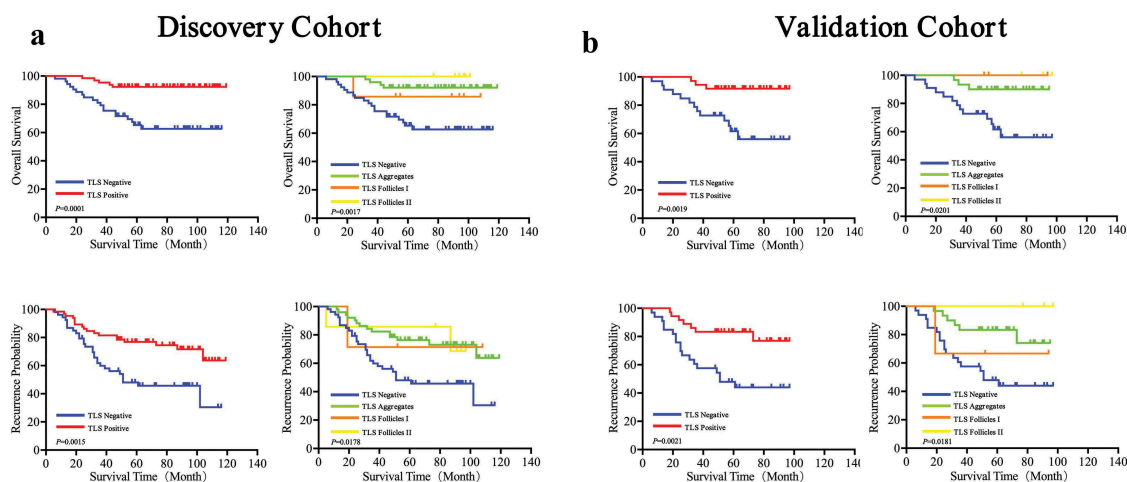


Figure 4. Prognostic significance of TLS phenotypes of in GIST patients.

(a). Kaplan-Meier analysis of overall survival (OS) and time to recurrence (TTR) in discovery cohort according to TLS phenotypes (n = 118). (b). Kaplan-Meier analysis of OS and TTR in validation cohort according to TLS phenotypes (n = 69).

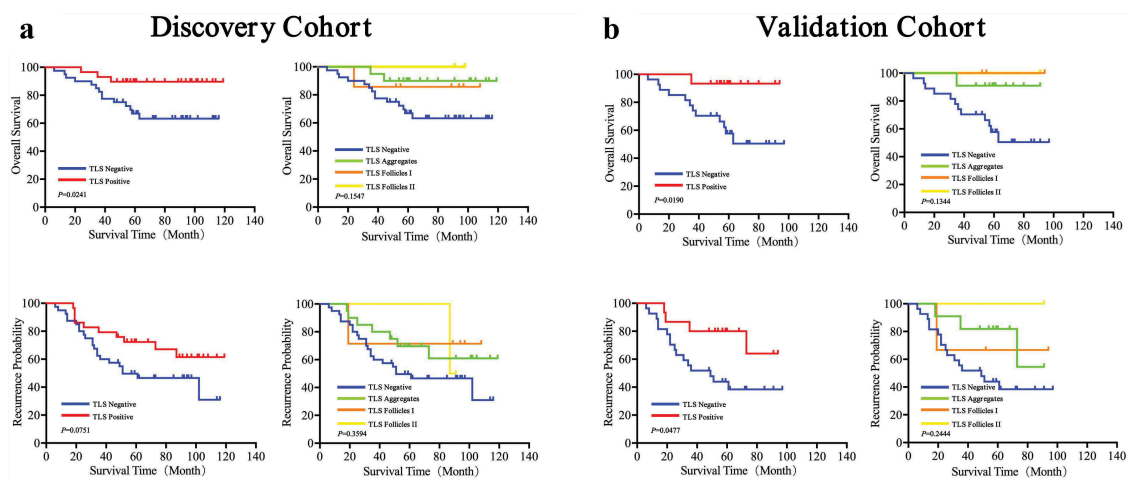


Figure 5. Prognostic significance of TLS phenotypes in GIST patients with the history of postoperative imatinib usage.

(a). Kaplan-Meier analysis of overall survival (OS) and time to recurrence (TTR) in discovery cohort according to TLS phenotypes (n = 69). (b). Kaplan-Meier analysis of OS and TTR in validation cohort according to TLS phenotypes (n = 42).

accounted for the majority while Treg cells, Th1 cells, Th2 cells, Th17 cells, PCs, Bn cells, IgM⁺ Bm cells, CD27⁻ Sw Bm cells and CD27⁺ Sw Bm cells accounted for a small percentage. We then analyzed the immune profiles in TLS⁺ and TLS⁻ patients. TLS⁺ patients had a higher number of B cells and a lower number of Treg cells in the intra-tumor regions. B cells localized in the TLS were observed to have high expression levels of activation-induced deaminase (AID), BCL-6 and activation of isotypic switch machinery, which are responsible for the generation of effector B cells differentiating into plasma cells and memory B cells to maintain a long-term immune response.³⁵ Furthermore, PD-1^{hi}CD8⁺ T cells, PD-1^{hi}CD4⁺ T_{FH} cells and DC-LAMP⁺ DCs were observed in the follicular B cell zone of TLS.^{40,44} This likely indicated an essential role of the TLS in promoting an interaction of T and B cells to generate an effective anti-tumor response.^{40,44}

Imatinib significantly improves the prognosis of GIST patients,¹¹ however, imatinib resistance is an inevitable

consequence. Hence, we analyzed the relationship between TLS and imatinib resistance. Surprisingly, we found that patients with TLS were less likely to develop imatinib resistance, indicating that the immune system could influence the development of imatinib resistance. In addition, we analyzed the immune profiles of TLS in imatinib-resistant and non-imatinib resistant patients. We observed that patients with imatinib resistance had a larger number of Treg and B cells and a lower number of CD8⁺ T cells in the TLS. This further demonstrated that immune cells were responsible for the development of imatinib resistance. Additional studies are needed to determine whether targeting the immune system could be a strategy to avoid imatinib resistance.

Immune checkpoint therapy, which has achieved a great success in lung cancer⁴⁵ and melanomas,⁴⁶ is thought to be effective in microsatellite instable patients.⁴⁷ Tumors with high TILs are thought to be a good predictor for sensitivity to immune checkpoint therapies, as they could promote *in situ* anti-tumor response and reverse immune escape

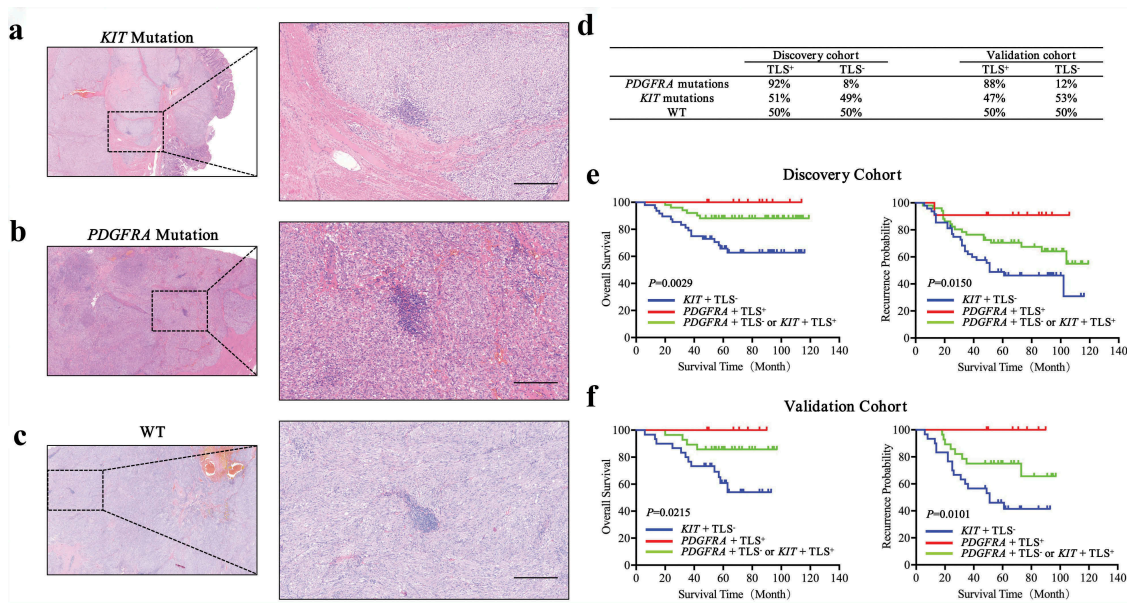


Figure 6. Association of mutation status with TLS phenotype in GIST patients.

(a). Representative H&E images in *KIT* mutation patients. Scale bar: 40 μ m (left), 200 μ m (right). (b). Representative H&E images in *PDGFRA* mutation patients. Scale bar: 40 μ m (left), 200 μ m (right). (c). Representative H&E images in WT patients. Scale bar: 40 μ m (left), 200 μ m (right). (d). The percentages of TLS positive patients and TLS negative patients in different mutation status in discovery cohort and validation cohort. (e). Kaplan-Meier analysis of OS (left) and TTR (right) in patients with group III: *KIT* mutation and TLS⁻ (blue), group I: *PDGFRA* mutation and TLS⁺ (red), group II: others (green) in discovery cohort. (f). Kaplan-Meier analysis of OS (left) and TTR (right) in patients with group III: *KIT* mutation and TLS⁻ (blue), group I: *PDGFRA* mutation and TLS⁺ (red), group II: others (green) in validation cohort.

mechanisms.²⁴ Therapies to block PD-1 and PD-L1, which could rescue exhausted CD8⁺ T cells via the PI3 K/Akt/mTOR signaling pathway,⁴⁸ had shown promising results in combination with imatinib for treating GIST.⁴⁹ Depending on CD8⁺ T cells, the combination of anti-CD40 drugs and imatinib has also been an effective strategy for treating GIST patients.⁵⁰ The combination of antiangiogenic and anti-PD-L1 therapies have been shown to increase TLS formation in breast and neuroendocrine pancreatic cancer patients.⁵¹ In contrast, caution is advised when administrating corticosteroids to manage chemotherapy side effects, as it could decrease the density of TLS in patients with lung squamous cell carcinomas.⁵² These findings are valuable to help us develop immunotherapies that specifically enables the formation of TLS to improve the prognosis of patients with GIST.

It is reported that the genomic alterations are associated with anti-tumor immunity and tumor mutation burdens, by promoting the generation of tumor neo-antigens, which is thought to be a major origin of adaptive immune responses.^{47,53,54} In patients with stage II/III non-metastatic colorectal carcinoma (nmCRC), TLS has been shown to be significantly associated with high-microsatellite-instability (MSI-H) and BRAF-mutant nmCRC, which may be through the production of immunogenic epitopes.⁵⁵ The presence of gene mutations is an important characteristic associated with GIST patients. We analyzed the combinational effects of these mutations and TLS in clinical outcomes. To our surprise, patients with *PDGFRA* mutations and positive TLS had the best prognosis for OS and TTR, while patients with *KIT* mutations and negative TLS had the worst prognosis for OS and TTR. The reason may be that patients with *PDGFRA* mutations are more likely to be TLS positive. This is consistent with

a previous study that demonstrated immune cells were more numerous and had higher cytolytic activity in *PDGFRA*-mutant GISTs compared to *KIT*-mutant GISTs.⁵⁶

Despite of the promising result, we still had some limitations in our study. Unfortunately, we did not have any results referring to the mechanism why TLS could influence the imatinib resistance and prognosis of GIST. Additional studies are required to determine how TLS originates and the exact role of TLS in the tumor microenvironment.

In conclusion, our present study demonstrated that the presence of tumor-infiltrating TLS was an independent prognostic factor for both OS and TTR. Furthermore, TLS was associated with lower imatinib resistance, longer survival and recurrence time after surgery. This indicated that TLS may have active anti-tumor activity and prevent anti-imatinib resistance. As drug resistance is becoming a severe problem for the treatment of patients with GIST, additional studies are urgently needed to determine whether patients with TLS could benefit from immune therapy or whether TLS could be induced to extend GIST patient survival.

Acknowledgements

We thank Pro. Hou and Liu for their help in diagnosing GIST in our patient cohorts as well as classifying TLS into different categories.

Disclosure of potential conflicts of interest

No potential conflicts of interest were disclosed.

Funding

This work was supported by the National Natural Science Foundation of China (81802302 from Ma LJ, 81871934 and 81572308 from Xue RY).

References

- Miettinen M, Lasota J. Gastrointestinal stromal tumors: pathology and prognosis at different sites. *Semin Diagn Pathol.* 2006;23(2):70–83. doi:10.1053/j.semdp.2006.09.001.
- Barnett CM, Corless CL, Heinrich MC. Gastrointestinal stromal tumors: molecular markers and genetic subtypes. *Hematol Oncol Clin North Am.* 2013;27(5):871–888. doi:10.1016/j.hoc.2013.07.003.
- Nilsson B, Bummig P, Meis-Kindblom JM, Odén A, Dortok A, Gustavsson B, Sablinska K, Kindblom L-G. Gastrointestinal stromal tumors: the incidence, prevalence, clinical course, and prognostication in the preimatinib mesylate era—a population-based study in western Sweden. *Cancer.* 2005;103(4):821–829. doi:10.1002/cncr.20862.
- Miettinen M, Lasota J. Gastrointestinal stromal tumors (GISTs): definition, occurrence, pathology, differential diagnosis and molecular genetics. *Pol J Pathol.* 2003;54:3–24.
- Miettinen M, Sobin LH, Lasota J. Gastrointestinal stromal tumors of the stomach: a clinicopathologic, immunohistochemical, and molecular genetic study of 1765 cases with long-term follow-up. *Am J Surg Pathol.* 2005;29(1):52–68. doi:10.1097/01.pas.0000146010.92933.de.
- Hirota S, Isozaki K, Moriyama Y, Nishida T, Ishiguro S, Kawano K, Hanada M, Kurata A, Takeda M, Tunio GM. Gain-of-function mutations of c-kit in human gastrointestinal stromal tumors. *Science (New York, NY).* 1998;279(5350):577–580. doi:10.1126/science.279.5350.577.
- Heinrich MC, Corless CL, Duensing A, McGreevey L, Chen CJ, Joseph N, Singer S, Griffith DJ, Haley A, Town A, Demetri GD. PDGFRA activating mutations in gastrointestinal stromal tumors. *Science (New York, NY).* 2003;299(5607):708–710. doi:10.1126/science.1079666.
- Joensuu H, Roberts PJ, Sarlomo-Rikala M, Andersson LC, Tervahartiala P, Tuveson D, Silberman SL, Capdeville R, Dimitrijevic S, Druker B, et al. Effect of the tyrosine kinase inhibitor STI571 in a patient with a metastatic gastrointestinal stromal tumor. *N Engl J Med.* 2001;344(14):1052–1056. doi:10.1056/NEJM200104053441404.
- Trent JC, Subramanian MP. Managing GIST in the imatinib era: optimization of adjuvant therapy. *Expert Rev Anticancer Ther.* 2014;14(12):1445–1459. doi:10.1586/14737140.2014.952284.
- Cheng CT, Tsai CY, Yeh CN, Chiang K-C, Chen -Y-Y, Wang S-Y, Chen T-W, Tseng J-H, Jung S-M, Chen T-C, et al. Clinical significance of pathological complete response in patients with metastatic gastrointestinal stromal tumors after imatinib mesylate treatment—lessons learned. *Anticancer Res.* 2014;34(11):6617–6625.
- Verweij J, Casali PG, Zalcberg J, LeCesne A, Reichardt P, Blay J-Y, Issels R, van Oosterom A, Hogendoorn PC, Van Glabbeke M, et al. Progression-free survival in gastrointestinal stromal tumours with high-dose imatinib: randomised trial. *Lancet (London, England).* 2004;364(9440):1127–1134. doi:10.1016/S0140-6736(04)17098-0.
- Joensuu H, Hohenberger P, Corless CL. Gastrointestinal stromal tumour. *Lancet (London, England).* 2013;382(9896):973–983. doi:10.1016/S0140-6736(13)60106-3.
- Demetri GD, van Oosterom AT, Garrett CR, Blackstein ME, Shah MH, Verweij J, McArthur G, Judson IR, Heinrich MC, Morgan JA, et al. Efficacy and safety of sunitinib in patients with advanced gastrointestinal stromal tumour after failure of imatinib: a randomised controlled trial. *Lancet (London, England).* 2006;368(9544):1329–1338. doi:10.1016/S0140-6736(06)69446-4.
- Demetri GD, Reichardt P, Kang YK, Blay J-Y, Rutkowski P, Gelderblom H, Hohenberger P, Leahy M, von Mehren M, Joensuu H, et al. Efficacy and safety of regorafenib for advanced gastrointestinal stromal tumours after failure of imatinib and sunitinib (GRID): an international, multicentre, randomised, placebo-controlled, phase 3 trial. *Lancet (London, England).* 2013;381(9863):295–302. doi:10.1016/S0140-6736(12)61857-1.
- Sautes-Fridman C, Lawand M, Giraldo NA, Kaplon H, Germain C, Fridman WH, Dieu-Nosjean M-C. Tertiary lymphoid structures in cancers: prognostic value, regulation, and manipulation for therapeutic intervention. *Front Immunol.* 2016;7:407. doi:10.3389/fimmu.2016.00407.
- Dieu-Nosjean MC, Goc J, Giraldo NA, Sautes-Fridman C, Fridman WH. Tertiary lymphoid structures in cancer and beyond. *Trends Immunol.* 2014;35(11):571–580. doi:10.1016/j.it.2014.09.006.
- Di Caro G, Marchesi F. Tertiary lymphoid tissue: A gateway for T cells in the tumor microenvironment. *Oncoimmunology.* 2014;3:e28850. doi:10.4161/onci.28850.
- de Chaisemartin L, Goc J, Damotte D, Validire P, Magdeleinat P, Alifano M, Cremer I, Fridman W-H, Sautes-Fridman C, Dieu-Nosjean M-C, et al. Characterization of chemokines and adhesion molecules associated with T cell presence in tertiary lymphoid structures in human lung cancer. *Cancer Res.* 2011;71(20):6391–6399. doi:10.1158/0008-5472.CAN-11-0952.
- Di Caro G, Bergomas F, Grizzi F, Doni A, Bianchi P, Malesci A, Laghi L, Allavena P, Mantovani A, Marchesi F, et al. Occurrence of tertiary lymphoid tissue is associated with T-cell infiltration and predicts better prognosis in early-stage colorectal cancers. *Clin Cancer Res.* 2014;20(8):2147–2158. doi:10.1158/1078-0432.CCR-13-2590.
- Dieu-Nosjean MC, Antoine M, Danel C, Heudes D, Wislez M, Poulot V, Rabbe N, Laurans L, Tartour E, de Chaisemartin L, et al. Long-term survival for patients with non-small-cell lung cancer with intratumoral lymphoid structures. *J Clin Oncol.* 2008;26(27):4410–4417. doi:10.1200/JCO.2007.15.0284.
- Hiraoka N, Ino Y, Yamazaki-Itoh R, Kanai Y, Kosuge T, Shimada K. Intratumoral tertiary lymphoid organ is a favourable prognosticator in patients with pancreatic cancer. *Br J Cancer.* 2015;112(11):1782–1790. doi:10.1038/bjc.2015.145.
- Martinet L, Garrido I, Filleron T, Le Guellec S, Bellard E, Fournie -J-J, Rochaix P, Girard J-P. Human solid tumors contain high endothelial venules: association with T- and B-lymphocyte infiltration and favorable prognosis in breast cancer. *Cancer Res.* 2011;71(17):5678–5687. doi:10.1158/0008-5472.CAN-11-0431.
- Ladanyi A, Kiss J, Somlai B, Gilde K, Fejős Z, Mohos A, Gaudi I, Tímár J. Density of DC-LAMP+ mature dendritic cells in combination with activated T lymphocytes infiltrating primary cutaneous melanoma is a strong independent prognostic factor. *Cancer Immunol Immunother.* 2007;56(9):1459–1469. doi:10.1007/s00262-007-0286-3.
- Calderaro J, Petitprez F, Becht E, Laurent A, Hirsch TZ, Rousseau B, Luciani A, Amaddeo G, Derman J, Charpy C, et al. Intra-tumoral tertiary lymphoid structures are associated with a low risk of early recurrence of hepatocellular carcinoma. *J Hepatol.* 2019;70(1):58–65. doi:10.1016/j.jhep.2018.09.003.
- Hou YY, Lu SH, Zhou Y, Qi W-D, Shi Y, Tan Y-S, Zhu X-Z. Stage and histological grade of gastrointestinal stromal tumors based on a new approach are strongly associated with clinical behaviors. *Mod Pathol.* 2009;22(4):556–569. doi:10.1038/modpathol.2009.11.
- Park SL, Gebhardt T, Mackay LK. Tissue-resident memory T cells in cancer immunosurveillance. *Trends Immunol.* 2019;40(8):735–747. doi:10.1016/j.it.2019.06.002.
- Nakayama T, Hirahara K, Onodera A, Endo Y, Hosokawa H, Shinoda K, Tumes DJ, Okamoto Y. Th2 cells in health and disease. *Annu Rev Immunol.* 2017;35:53–84. doi:10.1146/annurev-immunol-051116-052350.
- Kroeger DR, Milne K, Nelson BH. Tumor-infiltrating plasma cells are associated with tertiary lymphoid structures, cytolytic T-cell responses, and superior prognosis in ovarian cancer. *Clin Cancer Res.* 2016;22(12):3005–3015. doi:10.1158/1078-0432.CCR-15-2762.
- Joensuu H, Wardelmann E, Sihto H, Eriksson M, Hall KS, Reichardt A, Hartmann JT, Pink D, Cameron S, Hohenberger P, Al-Batran SE. Effect of KIT and PDGFRA mutations on survival

- in patients with gastrointestinal stromal tumors treated with adjuvant imatinib: An Exploratory Analysis of a Randomized Clinical Trial. *JAMA Oncol.* **2017**;3(5):602–609. doi: 10.1001/jamaoncol.2016.5751.
30. Fridman WH, Zitvogel L, Sautes-Fridman C, Kroemer G. The immune contexture in cancer prognosis and treatment. *Nat Rev Clin Oncol.* **2017**;14(12):717–734. doi:10.1038/nrclinonc.2017.101.
 31. Aloisi F, Pujol-Borrell R. Lymphoid neogenesis in chronic inflammatory diseases. *Nat Rev Immunol.* **2006**;6(3):205–217. doi:10.1038/nri1786.
 32. Carragher DM, Rangel-Moreno J, Randall TD. Ectopic lymphoid tissues and local immunity. *Semin Immunol.* **2008**;20(1):26–42. doi:10.1016/j.smim.2007.12.004.
 33. Goc J, Germain C, Vo-Bourgais TK, Lupo A, Klein C, Knockaert S, de Chaisemartin L, Ouakrim H, Becht E, Alifano M, et al. Dendritic cells in tumor-associated tertiary lymphoid structures signal a Th1 cytotoxic immune contexture and license the positive prognostic value of infiltrating CD8+ T cells. *Cancer Res.* **2014**;74(3):705–715. doi:10.1158/0008-5472.CAN-13-1342.
 34. Liu X, Tsang JYS, Hlaing T, Hu J, Ni Y-B, Chan SK, Cheung SY, Tse GM. Distinct tertiary lymphoid structure associations and their prognostic relevance in HER2 positive and negative breast cancers. *Oncologist.* **2017**;22(11):1316–1324. doi:10.1634/theoncologist.2017-0029.
 35. Sautes-Fridman C, Petitprez F, Calderaro J, Fridman WH. Tertiary lymphoid structures in the era of cancer immunotherapy. *Nat Rev Cancer.* **2019**;19(6):307–325. doi:10.1038/s41568-019-0144-6.
 36. Eroglu Z, Zaretsky JM, Hu-Lieskovan S, Kim DW, Algazi A, Johnson DB, Liniker E, Kong B, Munhoz R, Rapisuwon S, et al. High response rate to PD-1 blockade in desmoplastic melanomas. *Nature.* **2018**;553(7688):347–350. doi:10.1038/nature25187.
 37. Sautes-Fridman C, Fridman WH. TLS in tumors: what lies within. *Trends Immunol.* **2016**;37(1):1–2. doi:10.1016/j.it.2015.12.001.
 38. Joshi NS, Akama-Garren EH, Lu Y, Lee D-Y, Chang G, Li A, DuPage M, Tammela T, Kerper N, Farago A, et al. Regulatory T cells in tumor-associated tertiary lymphoid structures suppress anti-tumor T cell responses. *Immunity.* **2015**;43(3):579–590. doi:10.1016/j.immuni.2015.08.006.
 39. Mellman I, Coukos G, Dranoff G. Cancer immunotherapy comes of age. *Nature.* **2011**;480(7378):480–489. doi:10.1038/nature10673.
 40. Montfort A, Pearce O, Maniati E, Vincent BG, Bixby L, Böhm S, Dowe T, Wilkes EH, Chakravarty P, Thompson R, et al. A strong B-cell response is part of the immune landscape in human high-grade serous ovarian metastases. *Clin Cancer Res.* **2017**;23(1):250–262. doi:10.1158/1078-0432.CCR-16-0081.
 41. Prilliman KR, Lemmens EE, Palioungas G, Wolfe TG, Allison JP, Sharpe AH, Schoenberger SP. Cutting edge: a crucial role for B7-CD28 in transmitting T help from APC to CTL. *J Immunol (Baltimore, Md: 1950).* **2002**;169(8):4094–4097. doi:10.4049/jimmunol.169.8.4094.
 42. Schoenberger SP, Toes RE, van der Voort EI, Offringa R, Melief CJ. T-cell help for cytotoxic T lymphocytes is mediated by CD40-CD40L interactions. *Nature.* **1998**;393(6684):480–483. doi:10.1038/31002.
 43. Bennett SR, Carbone FR, Karamalis F, Flavell RA, Miller JF, Heath WR. Help for cytotoxic-T-cell responses is mediated by CD40 signalling. *Nature.* **1998**;393(6684):478–480. doi:10.1038/30996.
 44. Thommen DS, Koelzer VH, Herzig P, Roller A, Trefny M, Dimeloe S, Kiialainen A, Hanhart J, Schill C, Hess C, et al. A transcriptionally and functionally distinct PD-1(+) CD8(+) T cell pool with predictive potential in non-small-cell lung cancer treated with PD-1 blockade. *Nat Med.* **2018**;24(7):994–1004. doi:10.1038/s41591-018-0057-z.
 45. Chen R, Tao Y, Xu X, Shan L, Jiang H, Yin Q, Pei L, Cai F, Ma L, Yu Y, et al. The efficacy and safety of nivolumab, pembrolizumab, and atezolizumab in treatment of advanced non-small cell lung cancer. *Discov Med.* **2018**;26(143):155–166.
 46. Franklin C, Livingstone E, Roesch A, Schilling B, Schadendorf D. Immunotherapy in melanoma: recent advances and future directions. *Eur J Sur Oncol.* **2017**;43(3):604–611. doi:10.1016/j.ejso.2016.07.145.
 47. Le DT, Uram JN, Wang H, Bartlett BR, Kemberling H, Eyring AD, Skora AD, Luber BS, Azad NS, Laheru D, et al. PD-1 blockade in tumors with mismatch-repair deficiency. *N Engl J Med.* **2015**;372(26):2509–2520. doi:10.1056/NEJMoa1500596.
 48. Zhao Y, Song Y, Wang Y, Huang Y, Li Z, Cui Y, Yi M, Xia L, Zhuang W, Wu X, et al. PD-1/PD-L1 blockade rescue exhausted CD8+ T cells in gastrointestinal stromal tumours via the PI3K/Akt/mTOR signalling pathway. *Cell Prolif.* **2019**;52(3):e12571. doi:10.1111/cpr.12571.
 49. Seifert AM, Zeng S, Zhang JQ, Kim TS, Cohen NA, Beckman MJ, Medina BD, Maltbaek JH, Loo JK, Crawley MH, et al. PD-1/PD-L1 blockade enhances T-cell activity and antitumor efficacy of imatinib in gastrointestinal stromal tumors. *Clin Cancer Res.* **2017**;23(2):454–465. doi:10.1158/1078-0432.CCR-16-1163.
 50. Zhang JQ, Zeng S, Vitiello GA, Seifert AM, Medina BD, Beckman MJ, Loo JK, Santamaria-Barria J, Maltbaek JH, Param NJ, et al. Macrophages and CD8(+) T cells mediate the antitumor efficacy of combined CD40 ligation and imatinib therapy in gastrointestinal stromal tumors. *Cancer Immunol Res.* **2018**;6(4):434–447. doi:10.1158/2326-6066.CIR-17-0345.
 51. Allen E, Jabouille A, Rivera LB, Lodewijckx I, Missiaen R, Steri V, Feyen K, Tawney J, Hanahan D, Michael IP, Bergers G. Combined antiangiogenic and anti-PD-L1 therapy stimulates tumor immunity through HEV formation. *Sci Transl Med.* **2017**;9(385). doi:10.1126/scitranslmed.aak9679.
 52. Silina K, Soltermann A, Attar FM, Casanova R, Uckelej ZM, Thut H, Wandres M, Isaievs S, Cheng P, Curioni-Fontecedro A, et al. Germinal centers determine the prognostic relevance of tertiary lymphoid structures and are impaired by corticosteroids in lung squamous cell carcinoma. *Cancer Res.* **2018**;78(5):1308–1320. doi:10.1158/0008-5472.CAN-17-1987.
 53. McGranahan N, Furness AJ, Rosenthal R, Ramskov S, Lyngaa R, Saini SK, Jamal-Hanjani M, Wilson GA, Birkbak NJ, Hiley CT, et al. Clonal neoantigens elicit T cell immunoreactivity and sensitivity to immune checkpoint blockade. *Science (New York, NY).* **2016**;351(6280):1463–1469. doi:10.1126/science.aaf1490.
 54. Rooney MS, Shukla SA, Wu CJ, Getz G, Hacohen N. Molecular and genetic properties of tumors associated with local immune cytolytic activity. *Cell.* **2015**;160(1–2):48–61. doi:10.1016/j.cell.2014.12.033.
 55. Posch F, Silina K, Leibl S, Mündlein A, Moch H, Siebenhüner A, Samaras P, Riedl J, Stotz M, Szkandera J, et al. Maturation of tertiary lymphoid structures and recurrence of stage II and III colorectal cancer. *Oncoimmunology.* **2018**;7(2):e1378844. doi:10.1080/2162402X.2017.1378844.
 56. Vitiello GA, Bowler TG, Liu M, Medina BD, Zhang JQ, Param NJ, Loo JK, Goldfeder RL, Chibon F, Rossi F, et al. Differential immune profiles distinguish the mutational subtypes of gastrointestinal stromal tumor. *J Clin Invest.* **2019**;129(5):1863–1877. doi:10.1172/JCI124108.